A Filter Bank for the Directional Decomposition of Images: Theory and Design

Roberto H. Bamberger, *Member, IEEE*, and Mark J. T. Smith, *Senior Member, IEEE*

***Abstract*—This paper introduces a directionally oriented 2-D filter bank with the property that the individual channels may be critically sampled without loss of information. The passband regions of the component filters are wedge shaped and thus provide directional information. It is shown that these filter bank outputs may be maximally decimated to achieve a minimum sample representation in a way that permits the original signal to be exactly reconstructed. The paper discusses the theory for directional decomposition and the issues associated with maximum decimation and reconstruction. In addition, implementation issues are addressed where realizations based on both recursive and nonrecursive filters are considered.**

I. Introduction

FAN filters with directional sensitivity are important in practice and have been used for processing in the areas of robotics and computer vision [1], [2], seismology [3]–[6], linear feature detection and enhancement [7]–[9], and to some extent in image compression [10]–[17]. These decompositions are also useful in multisensor array processing problems where the data of interest are often plane waves propagating in a dispersive medium.

Similarly, filters for subband analysis/synthesis which allow a two-dimensional input signal to be represented by a sum of maximally decimated subband images and then reconstructed from these decimated images are also of great importance for image processing, primarily in the area of image coding [18]–[23]. In the past, much attention has been devoted to 1-D decimated filter banks and methods of reconstruction from the decimated channels. More recently, reconstruction methods for 2-D filter banks have received a great deal of attention. In these methods, the constituent filters are low pass, bandpass, and high pass. Maximum decimation and directional sensitivity are clearly useful filter bank properties and to date have only been treated separately. This paper presents a new 2-D filter bank which explicitly combines these two properties. The new filter bank decomposes images into directional components which can be maximally decimated while still allowing the original image to be exactly reconstructed from its decimated channels. The fan filters employed in this new filter bank have wedge-shaped passband spectral regions as shown in Fig. 1. It is easily shown (see [24]) that these wedge-shaped regions correspond to directional components of the image. Furthermore, if the filter bank is designed so that the filter passbands are narrow slivers in the 2-D Fourier domain, the filter bank channels can be related to the discrete Radon transform (DRT). The precise nature of this relationship is discussed in [25]. A filter bank with these directional properties is expected to have application in several areas, including determining the direction of arrival of a plane wave and the removal of ground roll in seismic processing [26], enhancement of linear features in noisy environments [9], [8], and image coding [27], [15].

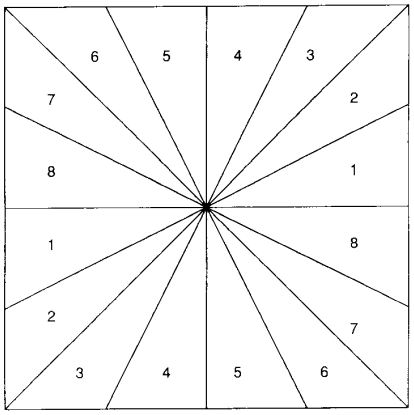

Fig. 1. Eight-band directional partitioning.

In order to achieve this decomposition in a computationally efficient manner, the filter bank can be implemented in a polyphase form. The polyphase filter bank is composed of simple modulators, polyphase filters, adders, delays, and upsamplers and downsamplers. In part, this efficiency is achieved by exploiting a property of generalized separability. Separable two-dimensional filter banks which have been discussed in the context of subband image coding typically involve filtering the horizontal rows of the image and then filtering the columns of the resulting images. In this paper it is useful to use a generalization of the separability concept where 1-D filtering is performed along linearly independent directions in the

Manuscript received December 12, 1989; revised February 19, 1991. This work was supported in part by the National Science Foundation under Contract DCI-8611372 and in part by an IBM Faculty Grant.

R. H. Bamberger was with the School of Electrical Engineering, Georgia Institute of Technology, Atlanta, GA 30332. He is now with the School of Electrical Engineering and Computer Science, Washington State University, Pullman, WA 99164-2752.

M. J. T. Smith is with the School of Electrical Engineering, Georgia Institute of Technology, Atlanta, GA 30332.

IEEE Log Number 9106032.

1053-587X/92$03.00 © 1992 IEEE

image. As will be seen later in the paper, the filtering is performed along the horizontal and vertical directions when the polyphase form of the filter bank is used.

The paper begins with a brief introduction to the notation and the basic 2-D sampling rate alteration equations and structures. This is followed by a description of the design of the analysis/synthesis filters and the implementation of the directional filter bank in a tree-structure. Most notably, the design method in [28] is generalized to the design of the exact and near-exact reconstruction analysis/synthesis filters required by the filter bank. In this approach, the two-dimensional filters are constructed by applying transformations to the superposition of two-dimensional separable filters whose constituent one-dimensional filters were previously designed to satisfy exact/aliasing-free reconstruction constraints. It is easily shown that the filtering and reconstruction properties of the one-dimensional system are preserved in the directional filter bank. In addition, computationally efficient polyphase implementations of the two-band filter banks are presented and issues specific to filtering finite extent signals while conserving their spatial regions of support are discussed in the context of the directional filter bank. The paper concludes with some examples of the analysis/synthesis filters and filtered test images.

II. Two-Dimensional Multirate Processing

Matrix/vector notations have been used for the description of multirate operations in two dimensions [29]. These descriptions enable relationships for multirate operations to be expressed in a form which resembles that of their one-dimensional counterparts. A good treatment of this theory may be found in [30]–[33], [13]. To lay the ground for discussion, some notational conventions and definitions used in this paper are mentioned first.

The spatial domain is described by the two-point column vector $[n_1\ n_2]^T$ which henceforth will be denoted $\boldsymbol{n}$. This leads to compact expressions for the discrete-time Fourier transform

$$X(\boldsymbol{\omega}) = \sum_{\boldsymbol{n}\in\Re_I} x[\boldsymbol{n}]e^{-j\boldsymbol{\omega}^T\boldsymbol{n}} \tag{1}$$

where $\boldsymbol{\omega} = [\omega_1, \omega_2]^T$, and the z transform

$$X(\boldsymbol{z}) = \sum_{\boldsymbol{n}\in\Re_I} x[\boldsymbol{n}]\boldsymbol{z}^{-\boldsymbol{n}} \quad \text{where } \boldsymbol{z}^{\boldsymbol{n}} = z_1^{n_1}z_2^{n_2}. \tag{2}$$

Upsampling and downsampling, the fundamental components of multirate digital processing, can also be expressed compactly. The upsampling operation with input $x[\boldsymbol{n}]$ and output $x_u[\boldsymbol{n}]$, is defined as

$$x_u[\boldsymbol{n}] = \begin{cases} x[\Lambda^{-1}\boldsymbol{n}], & \Lambda^{-1}\boldsymbol{n} \in \Re_I \\ 0, & \text{otherwise} \end{cases} \tag{3}$$

where $\Re_I$ denotes the integer lattice of points. In other words, $x_u[\boldsymbol{n}]$ is formed by taking the samples of $x[\boldsymbol{n}]$ on the rectangular lattice and mapping them to the sublattice (Λ) (defined by $\Lambda\boldsymbol{n}$). The analogous Fourier transform relationship (derived in [30], [31], [29], [13]) is

$$X_u(\boldsymbol{\omega}) = X(\Lambda^T\boldsymbol{\omega}). \tag{4}$$

From an inspection of the Fourier relationship of (4), it is seen that the rectangular spectral region

$$\{-\pi \le \omega_1 \le \pi\} \cap \{-\pi \le \omega_2 \le \pi\} \tag{5}$$

is mapped to the parallelogram-shaped region

$$\{-\pi \le \lambda_{11}\omega_1 + \lambda_{21}\omega_2 \le \pi\} \cap \{-\pi \le \lambda_{12}\omega_1 + \lambda_{22}\omega_2 \le \pi\} \tag{6}$$

where

$$\Lambda = \begin{bmatrix} \lambda_{11} & \lambda_{12} \\ \lambda_{21} & \lambda_{22} \end{bmatrix}.$$

The process of low-pass interpolation is accomplished by first upsampling the signal and then extracting only the baseband replica of $x[\boldsymbol{n}]$ by filtering it with a low-pass filter with passband as specified by (6). Bandpass interpolation is achieved by shifting the passband in (6) by $2\pi(\Lambda^T)^{-1}\boldsymbol{k}_l$ where $\boldsymbol{k}_l$ is a coset vector, ($\boldsymbol{k}_l \in \Re_I$).

Similarly, downsamplers can be expressed compactly as

$$x_d[\boldsymbol{n}] = x[\mu\boldsymbol{n}] \tag{7}$$

where $x[\boldsymbol{n}]$ is mapped to $x_d[\boldsymbol{n}]$ by discarding all the samples of $x[\boldsymbol{n}]$ which do not lie on the sublattice(μ). In order to avoid aliasing, the signal to be downsampled is usually prefiltered with a suitable antialiasing filter. For clarity, the term decimation will always refer to a signal that has been filtered with an appropriate antialiasing filter and then downsampled. The Fourier transform relationship for (7), [31], [33], [13], is

$$X_d(\boldsymbol{\omega}) = \frac{1}{M}\sum_{l=0}^{M-1} X((\mu^T)^{-1}(\boldsymbol{\omega} - 2\pi\boldsymbol{k}_l)) \tag{8}$$

where the vectors $\boldsymbol{k}_l$ ($0 \le l \le M$) are the coset vectors and $M = |\det(\mu)|$.

Several points are noteworthy at this time. There are only $M = |\det(\mu)|$ distinct cosets for a given resampling matrix μ. In this paper, the coset vectors will always be chosen to be the set of integer vectors of shortest length which maps the sublattice(μ) to the M distinct cosets of μ. For notational convenience, the coset vector $\boldsymbol{k}_0$ will always be the zero vector. Decimation of the low-pass channel, which results in $X_d(\boldsymbol{\omega}) \simeq (1/M)X((\mu^T)^{-1}\boldsymbol{\omega})$, can be accomplished by first filtering the signal, $x[\boldsymbol{n}]$, with an antialiasing filter whose nominal passband is

$$\{-\pi \le \mu_{11}\omega_1 + \mu_{21}\omega_2 \le \pi\} \cap \{-\pi \le \mu_{12}\omega_1 + \mu_{22}\omega_2 \le \pi\} \tag{9}$$

and whose downsampling matrix μ is assumed to be

$$\mu = \begin{bmatrix} \mu_{11} & \mu_{12} \\ \mu_{21} & \mu_{22} \end{bmatrix}. \tag{10}$$

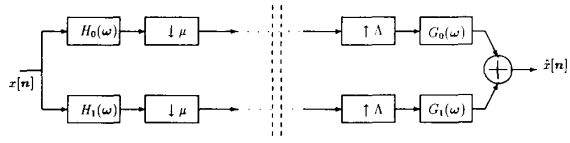

Fig. 2. Two-band structure.

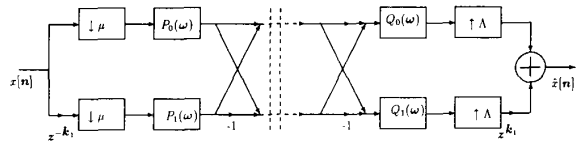

Fig. 3. Two-band polyphase structure.

With these multirate operations defined, the two-band filter bank structure shown in Fig. 2, the fundamental building block of the directional filter bank, can be analyzed conveniently. The analysis section of such structures decomposes a signal into its subband components by first filtering with a bank of bandpass filters, and then maximally downsampling the filtered outputs with a corresponding bank of downsamplers. The synthesis section reconstructs an approximation of the input by interpolating the subband signals and then recombining them. One issue of great concern in the design of multirate filter banks and image processing algorithms is computational efficiency. Inspection of the analysis section of the two-band structure shown in Fig. 2 reveals that the filtering operation always takes place at the original (higher) sampling rate and then half of the output samples are then discarded by the downsamplers.

Computation can be reduced by approximately 50% by using polyphase filter bank structures which achieve their computational savings by filtering the signal at the lower sampling rates and sharing the computational load between the high-pass and low-pass channels. There are several polyphase implementations possible [34]. The polyphase structure used in this work, shown in Fig. 3, is a special case of the more general polyphase structure presented in [34]. In order to share the computational load between the high-pass and low-pass channels, a certain amount of generality is sacrificed by restricting the high-pass and low-pass filters to be frequency shifted versions of each other. A simple analysis and comparison of the direct form (Fig. 2) and polyphase form (Fig. 3) indicates that the two systems are equivalent if and only if

$$H_0(\boldsymbol{\omega}) = P_0(\mu^T\boldsymbol{\omega}) + e^{-j\boldsymbol{\omega}^T k_1}P_1(\mu^T\boldsymbol{\omega})$$
$$H_1(\boldsymbol{\omega}) = P_0(\mu^T\boldsymbol{\omega}) - e^{-j\boldsymbol{\omega}^T k_1}P_1(\mu^T\boldsymbol{\omega}) \quad (11)$$
$$G_0(\boldsymbol{\omega}) = Q_0(\Lambda^T\boldsymbol{\omega}) + e^{j\boldsymbol{\omega}^T k_1}Q_1(\Lambda^T\boldsymbol{\omega})$$
$$G_1(\boldsymbol{\omega}) = Q_0(\Lambda^T\boldsymbol{\omega}) - e^{j\boldsymbol{\omega}^T k_1}Q_1(\Lambda^T\boldsymbol{\omega}) \quad (12)$$

where $P_0(\boldsymbol{\omega})$ and $P_1(\boldsymbol{\omega})$ are the polyphase analysis filters, and $Q_0(\boldsymbol{\omega})$ and $Q_1(\boldsymbol{\omega})$ are the polyphase synthesis filters. Further analysis shows that (11) and (12) require the following symmetry in the analysis/synthesis filters:

$$H_0(\boldsymbol{\omega}) = H_1(\boldsymbol{\omega} - (\mu^T)^{-1}\boldsymbol{k}_1 2\pi)$$
$$G_0(\boldsymbol{\omega}) = G_1(\boldsymbol{\omega} - (\Lambda^T)^{-1}\boldsymbol{k}_1 2\pi). \quad (13)$$

As is evident from (13), the frequency shift is completely defined by the resampling matrices and their coset vectors. These two-band structures (direct and polyphase) form the basic building block for the directional filter bank which is introduced in the next section.

III. The Directional Filter Bank

The proposed directional filter bank is implemented in a tree-structure composed of two-band systems. The most basic directional decomposition is a two-band split which divides a signal into the two hour-glass-shaped spectral regions depicted in Fig. 4. To maximally decimate the output of the hour-glass-shaped filters, it is desirable to modulate the signal by π in either the ω_1 or ω_2 frequency variable. Alternately, the input signal can first be modulated by π and then filtered with a filter pair which has the diamond-shaped characteristic shown in Fig. 5. As can be seen from (6) and (9), the resampling matrices corresponding to the diamond-shaped analysis/synthesis filters are given by

$$\mu = \Lambda = \begin{bmatrix} 1 & -1 \\ 1 & 1 \end{bmatrix}. \quad (14)$$

For a four-band decomposition, the second stage of the tree structure is identical to the first. A typical first or second stage of the filter bank is shown in Fig. 6. The remaining stages of the directional filter bank are composed of the simple two-band structures of Fig. 2. Due to geometrical constraints, the filters and resampling matrices for the remaining stages are not the same as the ones for the first two stages. Consider, for example, the 8-band decomposition of a signal where the desired spectral partitioning is shown in Fig. 1.

The first stage, a two-band split, results in one signal which contains components 1, 2, 7, and 8 of Fig. 1, and a signal which contains components 3, 4, 5, and 6. The next level in the tree structure, a four-band decomposition, yields four directional components. Fig. 7 shows where the spectral components in Fig. 1 are mapped by the 4 direction decomposition. An inspection of Fig. 7 reveals that in order to separate the spectral components labeled 1 and 2 from the outputs of the four-band decomposition, it is necessary to design a two-band filter bank whose analysis/synthesis filters have parallelogram-shaped passbands. A further analysis reveals that four different two-band structures are required for the desired 8-band decomposition, each having analysis/synthesis filters with parallelogram-shaped passbands. The four parallelogram-shaped characteristics required for the eight-band decomposition are shown in Fig. 8. Given the desired ideal passband characteristics, the corresponding re-

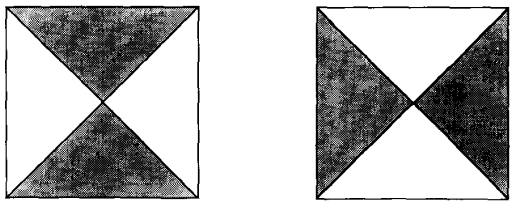

(a) (b)

Fig. 4. Hour-glass-shaped filter responses.

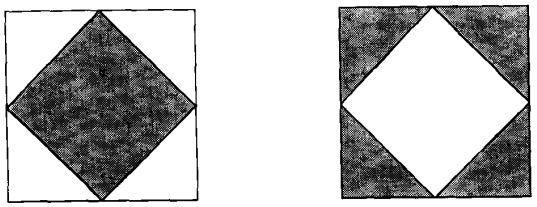

(a) (b)

Fig. 5. Ideal frequency response for diamond filter pair.

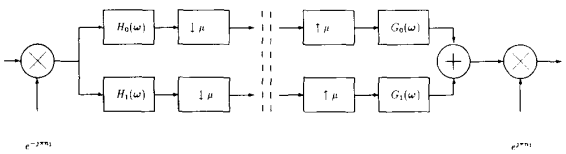

Fig. 6. Stages 1 and 2 for the directional filter bank.

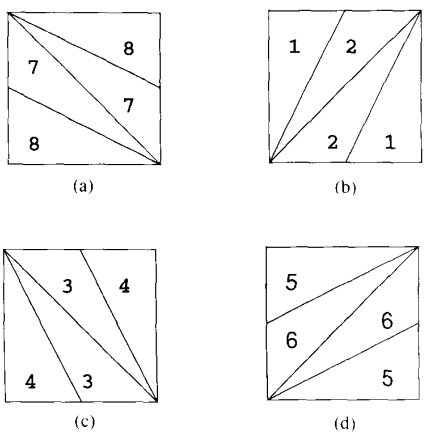

(a) (b) (c) (d)

Fig. 7. The locations of the spectral regions of the original 8-band desired spectral partitioning in the resulting subbands. (a) The output signal for low-pass stages 1 and 2, (b) low-pass stage 1, high-pass stage 2, (c) high-pass stage 1, and low-pass stage 2, (d) high-pass stage 1, high-pass stage 2.

sampling matrices are found by applying (9). In addition, it can be shown that for 16, 32, and in general any 2^N band decomposition, all the remaining two-band sections use only these four parallelogram-shaped filter characteristics.

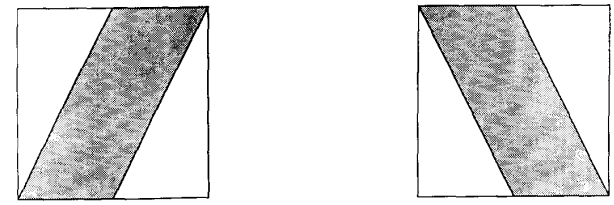

(a) (b)

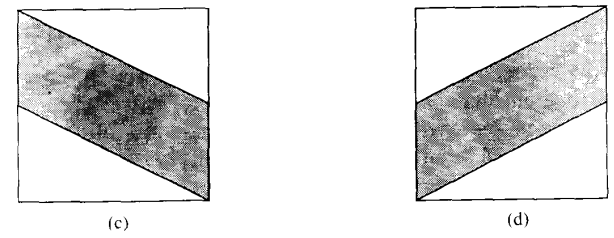

(c) (d)

Fig. 8. Ideal frequency responses for the parallelogram filters.

IV. Design of the Analysis Filters

Thus far, directional decomposition has been discussed using ideal filters. To implement the directional filter bank, it is necessary to design the 2-D analysis/synthesis filters. The design of practical 2-D analysis/synthesis filters can be achieved by employing 1-D filters and the concept of generalized separability. In [28], Ansari describes a method for designing efficient ninety degree FIR and IIR fan filters. In [35], the approach in [28] is used to design 2-D IIR analysis/synthesis filters with the diamond-shaped frequency response shown in Fig. 5. In this paper, a generalization of Ansari's method is presented that allows for the design of both the diamond and parallelogram-shaped filter banks. These filters may be either FIR and IIR. This design method provides a compact parameterization of the entire filter bank in terms of the 1-D prototype filter and the 2-D downsampling matrix for each desired geometry. It is further demonstrated that the two-band filters designed in this manner have the necessary symmetry to be implemented in the polyphase form of Fig. 3. Moreover, the resulting polyphase filters are rectangularly separable.

Up until this point, only the fundamental period of the filter responses have been shown. However, the filters are actually periodic with period 2π in both the ω_1 and ω_2 variables. Observing that the filter responses have this periodicity, it is revealed that all the filters, diamond and parallelogram-shaped passbands alike, have a checkerboard-shaped response which has been rotated, skewed, and/or scaled. The design methodology presented here uses a change of variables applied to the checkerboard-shaped responses shown in Fig. 9 to effect the rotation, skewing, and scaling necessary. Hence, there are two issues which must be addressed: a proper choice of change of variables and the design of the checkerboard-shaped filters shown in Fig. 9.

The change of variables is chosen to be

$$\begin{bmatrix} \omega_1' \\ \omega_2' \end{bmatrix} = \frac{\mu^T}{|\det(\mu)|} \begin{bmatrix} \omega_1 \\ \omega_2 \end{bmatrix} \tag{15}$$

where the matrix μ is the appropriate downsampling matrix for the desired geometry (diamond or parallelogram) passbands. Alternately, we can express the change of variables in terms of the z transform as

$$\begin{aligned} z_1' &= z_1^{\mu_{11}/2} z_2^{\mu_{21}/2} \\ z_2' &= z_1^{\mu_{12}/2} z_2^{\mu_{22}/2} \end{aligned} \tag{16}$$

where $|\det(\mu)| = 2$ since only two-band systems are being considered. This choice of change of variables provides the appropriate rotation, skewing, and scaling for all the filters required for the directional filter bank. This change of variables is a general one which will transform any filter with the checkerboard-shaped responses shown in Fig. 9 to filters with the geometry implied by (9). To ensure that the resultant filter banks have all the desired properties previously mentioned, care must be taken in the design of the checkerboard-shaped filters.

The checkerboard filter can be viewed as a sum of two square-shaped filters where one filter is equivalent to the other shifted by π in both the ω_1 and ω_2 directions. The first step in the design of these 2-D analysis filters is to select a one-dimensional filter pair such that

$$H_0(z) = H_1(-z). \tag{17}$$

The filters $H_0(z)$ and $H_1(z)$ are half-band low-pass and high-pass filters, respectively. This relationship between the 1-D filters allows $H_0(z)$ and $H_1(z)$ to be expressed in terms of their polyphase components

$$H_0(z) = P_0(z^2) + z^{-1}P_1(z^2) \tag{18}$$

$$H_1(z) = P_0(z^2) - z^{-1}P_1(z^2). \tag{19}$$

The square spectrum filters $B_0(z_1, z_2)$ and $B_1(z_1, z_2)$ can then be formed where

$$\begin{aligned} B_0(z_1, z_2) &= H_0(z_1)H_0(z_2) \\ B_1(z_1, z_2) &= H_0(z_1)H_1(z_2). \end{aligned} \tag{20}$$

The square spectrum filters in turn can be used to form the checkerboard patterned filters

$$\begin{aligned} C_0(z_1, z_2) &= B_0(z_1, z_2) + B_0(-z_1, -z_2) \\ C_1(z_1, z_2) &= B_1(z_1, z_2) + B_1(-z_1, -z_2). \end{aligned} \tag{21}$$

Equivalently, the checkerboard filters can be expressed in terms of the polyphase components of the original 1-D prototype filter

$$\begin{aligned} C_0(z_1, z_2) &= 2[P_0(z_1^2)P_0(z_2^2) + z_1^{-1}z_2^{-1}P_1(z_1^2)P_1(z_2^2)] \\ C_1(z_1, z_2) &= 2[P_0(z_1^2)P_0(z_2^2) - z_1^{-1}z_2^{-1}P_1(z_1^2)P_1(z_2^2)]. \end{aligned} \tag{22}$$

Applying the change of variables in (16) to the checkerboard filters $C_0(z_1, z_2)$ and $C_1(z_1, z_2)$ results in

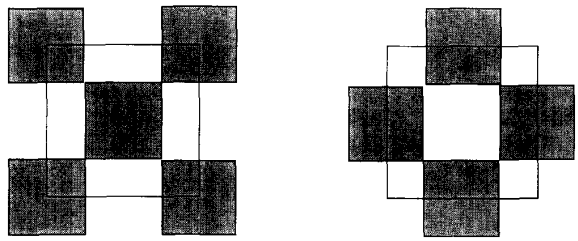

(a) (b)

Fig. 9. Ideal passband characteristics for the checkerboard-patterned filters (a) $C_0(z_1, z_2)$, and (b) $C_1(z_1, z_2)$.

$$\begin{aligned} D_0(z_1, z_2) &= C_0(z_1^{\mu_{11}/2}z_2^{\mu_{21}/2}, z_1^{\mu_{12}/2}z_2^{\mu_{22}/2}) \\ &= 2[P_0(z_1^{\mu_{11}}z_2^{\mu_{21}}, z_1^{\mu_{12}}z_2^{\mu_{22}}) \\ &\quad + z_1^{-(\mu_{11}+\mu_{12})/2}z_2^{-(\mu_{21}+\mu_{22})/2}P_1(z_1^{\mu_{11}}z_2^{\mu_{21}}, z_1^{\mu_{12}}z_2^{\mu_{22}})] \\ D_1(z_1, z_2) &= C_1(z_1^{\mu_{11}/2}z_2^{\mu_{21}/2}, z_1^{\mu_{12}/2}z_2^{\mu_{22}/2}) \\ &= 2[P_0(z_1^{\mu_{11}}z_2^{\mu_{21}}, z_1^{\mu_{12}}z_2^{\mu_{22}}) \\ &\quad - z_1^{-(\mu_{11}+\mu_{12})/2}z_2^{-(\mu_{21}+\mu_{22})/2}P_1(z_1^{\mu_{11}}z_2^{\mu_{21}}, z_1^{\mu_{12}}z_2^{\mu_{22}})] \end{aligned} \tag{23}$$

where the two-dimensional polyphase filters are defined as

$$\begin{aligned} P_0(z_1, z_2) &= P_0(z_1)P_0(z_2) \\ P_1(z_1, z_2) &= P_1(z_1)P_1(z_2). \end{aligned} \tag{24}$$

Rewriting (23) in the Fourier domain yields the required analysis filters:

$$\begin{aligned} D_0(\boldsymbol{\omega}) &= P_0(\mu^T\boldsymbol{\omega}) + \exp\left[-j\omega_1\left(\frac{\mu_{11}+\mu_{12}}{2}\right)\right] \\ &\quad \cdot \exp\left[-j\omega_2\left(\frac{\mu_{21}+\mu_{22}}{2}\right)\right] P_1(\mu^T\boldsymbol{\omega}) \\ D_1(\boldsymbol{\omega}) &= P_0(\mu^T\boldsymbol{\omega}) - \exp\left[-j\omega_1\left(\frac{\mu_{11}+\mu_{12}}{2}\right)\right] \\ &\quad \cdot \exp\left[-j\omega_2\left(\frac{\mu_{21}+\mu_{22}}{2}\right)\right] P_1(\mu^T\boldsymbol{\omega}). \end{aligned} \tag{25}$$

Comparing (11) and (25) reveals that not only are the resulting analysis filters implementable in the efficient polyphase structure of Fig. 3, but the resulting two-dimensional polyphase filters are rectangularly separable.

In addition to the nominal passband shape, the directional filter bank design problem calls for obtaining analysis/synthesis filters with prescribed passband ripples, stopband ripples, and transition bandwidths. Given such a set of analysis/synthesis filter specifications, it is possible to determine characteristics for the 1-D prototype filter needed for the design. The stopband ripple, δ_s', and passband ripple, δ_p', of the 2-D filter are independent of passband geometry and the associated change of variables. They are related to the 1-D prototype filter speci-

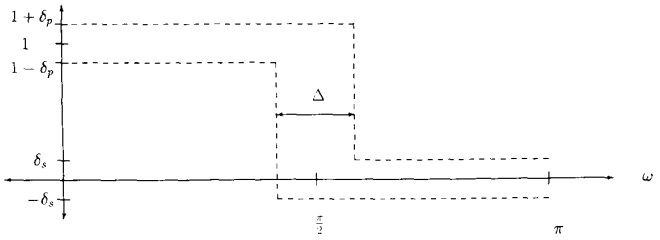

Fig. 10. One-dimensional prototype filter tolerances demonstrating δ_p, δ_s, and Δ.

fications by

$$\delta_s' = 2(1 + \delta_p)\,\delta_s$$
$$\delta_p' = 2\delta_p + \delta_p^2 + \delta_s^2 \tag{26}$$

where δ_s, and δ_p are the corresponding ripples in the 1-D filter as shown in Fig. 10. Given the desired values for δ_p' and δ_s', the equations in (26) can be used to find appropriate values of δ_p and δ_s. The transition bandwidth is dependent on the resampling matrix which defines the change of variables. Depending on the change of variables (resampling matrix), the resulting two-dimensional filters can have two different transition bandwidths, denoted Δ_1 and Δ_2. Careful analysis of the change of variables reveals that the resulting transition bandwidths are

$$\Delta_1 = (\mu_{11}^2 + \mu_{12}^2)^{1/2}\,\frac{\Delta}{2}$$
$$\Delta_2 = (\mu_{21}^2 + \mu_{22}^2)^{1/2}\,\frac{\Delta}{2} \tag{27}$$

where Δ is the transition bandwidth of the 1-D filter.

Now that the analysis filters have been designed, it is necessary to design the synthesis filters so that the filter bank provides exact/aliasing-free reconstruction. In the next section, a discussion of the reconstruction issues is presented. There it is shown that it is possible to exactly reconstruct the input in spite of the aliasing and filtering distortions, a result which previously has only been demonstrated for the class of filters used for subband image coding.

V. Reconstruction from Maximally Decimated Directional Channels

There exist many methods for designing exact/aliasing-free filter banks [36]–[41]. In particular, much of the theory has been developed in the context of 1-D filter banks and has recently been adapted to handle 2-D filter banks. A useful filter bank design and analysis tool is the AC matrix framework [36]. (Several 2-D filter bank design algorithms have been presented, and include [32], [42]–[45]. The extension of AC matrix theory to the 2-D case is presented in the Appendix. Using the 2-D AC matrix theory, many different filter banks can be conveniently analyzed and designed. For the two-band filter banks used in this paper, the result of this analysis is that aliasing-free reconstruction is achieved if the synthesis filters, $G_0(\omega)$ and $G_1(\omega)$, are

$$\begin{bmatrix} G_0(\omega) \\ G_1(\omega) \end{bmatrix} = \frac{D(\omega)}{\det\,(H_{AC})} \begin{bmatrix} H_1(\omega - (\mu^T)^{-1}\boldsymbol{k}_1 2\pi) \\ -H_0(\omega) - (\mu^T)^{-1}\boldsymbol{k}_1 2\pi) \end{bmatrix} \tag{28}$$

where $D(\omega)$ is the overall system frequency response and $\det\,(H_{AC})$ is as defined in the Appendix. Applying the AC matrix equations, two 2-D solutions become evident. The first is a direct extension of the classical 1-D QMF filters [39], while the second is based on using recursive allpass polyphase filters [46].

QMF filters are popular in 1-D and 2-D separable filter banks where aliasing cancellation is desired. The classical 1-D solution imposes the constraint

$$H_0(\omega) = H_1(\omega - \pi). \tag{29}$$

The analogous constraint in the general two-dimensional case is

$$H_0(\omega) = H_1(\omega - (\mu^T)^{-1}\boldsymbol{k}_1 2\pi) \tag{30}$$

which is the same symmetry required for a polyphase implementation. It is noteworthy that the symmetry condition of (30) is directly dependent on the downsampling matrix μ and hence its coset vector $\boldsymbol{k}_1$. The QMF solution is obtained by choosing

$$\begin{bmatrix} G_0(\omega) \\ G_1(\omega) \end{bmatrix} = \begin{bmatrix} H_1(\omega - (\mu^T)^{-1}\boldsymbol{k}_1 2\pi) \\ -H_0(\omega - (\mu^T)^{-1}\boldsymbol{k}_1 2\pi) \end{bmatrix}. \tag{31}$$

Comparing (31) and (28) results in a frequency distortion

$$D(\omega) = H_0^2(\omega) - H_1^2(\omega). \tag{32}$$

Close inspection reveals that if $H_0(\omega)$ closely matches the ideal frequency response specified by (9), then the filters can be designed so that the frequency distortion is negligible. Furthermore, it can be shown that if 1-D QMF filters are used in the design algorithm described in the previous section, then the resulting 2-D filters satisfy the symmetry constraints of (30). In the general case, the polyphase analysis filters for the multidimensional QMF filter bank are

$$p_0[\boldsymbol{n}] = h_0[\mu\boldsymbol{n}]$$
$$p_1[\boldsymbol{n}] = h_0[\mu\boldsymbol{n} + \boldsymbol{k}_1] \tag{33}$$

and the polyphase synthesis filters are

$$q_0[n] = p_1[n]$$
$$q_1[n] = p_0[n]. \tag{34}$$

In the special case discussed here, the polyphase analysis/synthesis filters are 2-D separable and thus are computationally efficient.

The directional filter banks can also be implemented using efficient recursive filters. It is well known that recursive digital filters generally have better magnitude characteristics than FIR filters of the same complexity. This efficiency has been exploited in one-dimensional filter banks in [40], [41], [47], [46] where some small amount of phase and/or frequency distortion is allowed. More recently it has been used in [23], [19], [20], where exact reconstruction 1-D IIR filter banks filters were shown to be effective for image coding. In these implementations the polyphase filters $P_0(z)$ and $P_1(z)$ are chosen to be all-pass filters of the form

$$P_0(z) = \prod_{i=1}^{M_0} \frac{z^{-1} - a_i}{1 - a_i z^{-1}}$$
$$P_1(z) = \prod_{i=1}^{M_1} \frac{z^{-1} - b_i}{1 - b_i z^{-1}} \tag{35}$$

where a_i and b_i are the poles of the analysis polyphase filters. The motivation for this choice is that all-pass filters of degree M can be performed very efficiently by taking advantage of the symmetry of the coefficients [46]. Thus the difference equation used to implement the filter requires only M multiplies and $2M$ adds per output sample.

As before, the synthesis filters needed to achieve exact reconstruction can be determined by using the synthesis (28) derived in the Appendix. To explore this approach further, we start with analysis filters $H_0(\omega)$ and $H_1(\omega)$ related by

$$H_0(\omega) = H_1(\omega - (\mu^T)^{-1}k_1 2\pi).$$

Applying the exact reconstruction expression given in (28), the exact reconstruction synthesis filters are

$$G_0(\omega) = \frac{2H_0(\omega)}{H_0^2(\omega) - H_1^2(\omega)}$$
$$G_1(\omega) = \frac{-2H_1(\omega)}{H_0^2(\omega) - H_1^2(\omega)}. \tag{36}$$

Substituting (11) (i.e., expressing $H_i(\omega)$ in terms of the polyphase filters) into the above expression and simplifying, yields

$$G_0(\omega) = \frac{1}{2}\left[\frac{1}{P_0(\mu^T\omega)} + \frac{e^{j\omega^T k_1}}{P_1(\mu^T\omega)}\right]$$
$$G_1(\omega) = \frac{1}{2}\left[\frac{1}{P_0(\mu^T\omega)} - \frac{e^{j\omega^T k_1}}{P_1(\mu^T\omega)}\right]. \tag{37}$$

Comparing the above equations to (12) and equating like terms reveals that the polyphase synthesis filters are simply the reciprocals of the analysis filters

$$Q_0(\omega) = \frac{1}{P_0(\omega)}$$
$$Q_1(\omega) = \frac{1}{P_1(\omega)}. \tag{38}$$

In this case, if the polyphase analysis filters are separable IIR all-pass filters, then the polyphase synthesis filters are also separable IIR all-pass filters. It should be noted that since the polyphase filters were chosen to be all-pass filters, stable causal polyphase analysis filters always result in anticausal stable polyphase synthesis filters. Thus, as long as the input images are finite in extent, system stability is not an issue. Other implementation issues are discussed in the following section.

VI. Implementation Issues

The sampling theorem implies that the directional space-frequency representation of an $N \times N$ image can be realized with a total of $N \times N$ samples. Therefore, an M-band directional decomposition can be uniquely represented with as few as N^2/M pixels in each band. However, this situation does not naturally arise in the system as described. If, for example, FIR analysis/synthesis filters are used, even with a maximally decimated filter bank, the total number of samples in the subband signals will be greater than the total number of samples in the original signal. The problem is even more evident for IIR filters where infinite samples result from filtering. Several solutions to the problem of obtaining a minimum sample representation are discussed in [19], [48]. A convenient solution is based on the periodic extension of the signal. It is easily shown that convolving a periodic sequence with periodicity matrix $\mathfrak{N}$,[1] with an aperiodic sequence results in a periodic sequence which also has periodicity matrix $\mathfrak{N}$. Therefore, if the finite extent sequence can be periodically replicated with a periodicity matrix $\mathfrak{N}$, then it is only necessary to retain one period of the filtered sequence which is a minimum sample representation.

Since only one period of the infinitely periodic filtered signal is retained, only one period need be computed. In the case of FIR filters, this is easily achieved using any of the direct form filter implementations [19]. For the IIR case, the filter is implemented as a difference equation and knowledge of the appropriate initial conditions is required. Since all the filtering in this paper is done with separable filters, the problem of computing the initial conditions is identical to the 1-D case. The closed form so-

[1] A two-dimensional signal is said to be periodic with periodicity matrix $\mathfrak{N}$ if

$$\tilde{x}[n + \mathfrak{N}_i] = \tilde{x}[n]$$

for $i = 1, 2$ and $\mathfrak{N} = [\mathfrak{N}_1\ \mathfrak{N}_2]$. Furthermore, if $\mathfrak{N}$ is diagonal, then $\tilde{x}[n]$ is said to be rectangularly periodic.

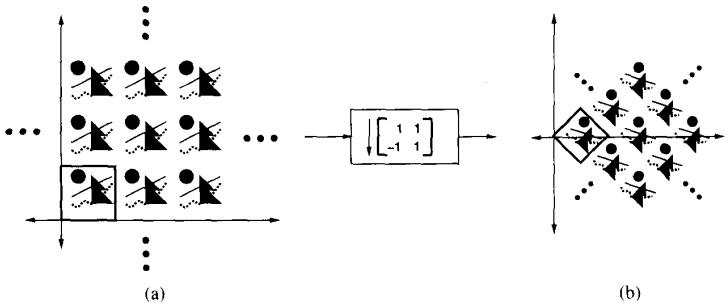

(a) (b)

Fig. 11. (a) Periodic extension of an input image, and (b) the resulting periodic image following downsampling. The fundamental period is shown in the outlined region.

lution for the one-dimensional case is presented in [19], [23] and is summarized here for completeness.

Consider a one-dimensional sequence $x[n]$ of length N and an all-pass filter $A(z)$ of order M where

$$A(z) = \prod_{i=1}^{M} \frac{z^{-1} - a_i}{1 - a_i z^{-1}}$$

and the poles of $A(z)$ are assumed to lie inside the unit circle. The periodic extension of $x[n]$ yields $\tilde{x}[n] = x[((n))_N]$ where $((n))_N$ denotes modulo division. After manipulating the difference equation for the IIR filter and making use of the periodicity of $\tilde{x}[n]$, the output of the filter can be written as

$$\tilde{y}[n] = A\tilde{x}[n] + \sum_{m=0}^{N-1} \tilde{x}[n - m] \sum_{i=1}^{M} \left(\frac{B_i}{1 - a_i^N} \right) a_i^m \quad (39)$$

where A and B_i are the partial fraction expansion coefficients of the all-pass filter, and the a_i's are the pole locations for the given filter. The above equation is then used to determine the initial conditions by evaluating the expression at $n = -1, -2, \cdots, -M$. Though (39) is a sum of N terms, it is often sufficient to evaluate the sum based on only the first few terms in the summation due to the exponential amplitude decay of the filter's impulse response.

In the implementation of the directional filter bank, some practical issues arise due to the periodic extension necessary for the filter bank to have the size limiting property. To fully understand these issues, it is first necessary to consider the effect of downsampling a signal $\tilde{x}[n]$ with periodicity $\mathfrak{N}$, by applying a downsampler μ. Applying the definition of the periodicity matrix $\mathfrak{N}$, it is easy to show that the output of the downsampler will have a periodicity of

$$\mathfrak{N}' = \mu^{-1}\mathfrak{N} \quad (40)$$

if $\mathfrak{N}'$ is a matrix containing only integer entries. An example of this phenomenon is shown in Fig. 11 where the change in periodicity is shown graphically for a particular μ. For storage efficiency, one fundamental period of the signal and its periodicity matrix are retained. It is important to note that for two-dimensional periodic signals,

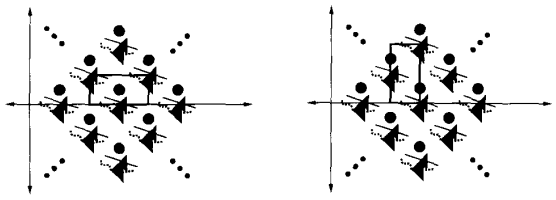

(a) (b)

Fig. 12. Alternate tilings. (a) Tiling used for periodically filtering rows of the signal, and (b) tiling used for periodically filtering columns of the signal. Again, the tiles are outlined.

there are an infinite number of choices for the fundamental period. Examples of two different fundamental periods which can be used to represent the image in Fig. 11(b) are shown in Fig. 12. The issue involved is that at each point in the implementation of the directional filter bank, a different choice of the fundamental period of the signal is required. Using the rectangularly separable polyphase implementation, the rows of the periodic sequence are filtered, followed by the columns of the result. This rectangularly separable filtering, in combination with the size-limiting nature of the filter bank requires that the rows and columns of the signals being filtered be periodic. For convenience, it is desirable that fundamental periods of the rows and columns be easily accessible. The choices of fundamental periods shown in Figs. 12(a) and (b) are appropriate for filtering the rows and columns of the image, respectively. It can be shown that a suitable tiling can always be found for each stage in the directional filter bank.

VII. Concluding Remarks

To illustrate this directionally based representation, the Cameraman image shown in Fig. 13, was used as a test input for decomposition. Fig. 14 shows the magnitude response of several different filter bank channels. This particular filter bank is based on separable, first-order all-pass polyphase filters and resolves the input into 16 directional components. An advantage of this recursive implementation is that each stage in the filter bank requires only 1 multiply and 2 additions per output sample. The

Fig. 13. Cameraman image (256 by 256 with 256 grey levels).

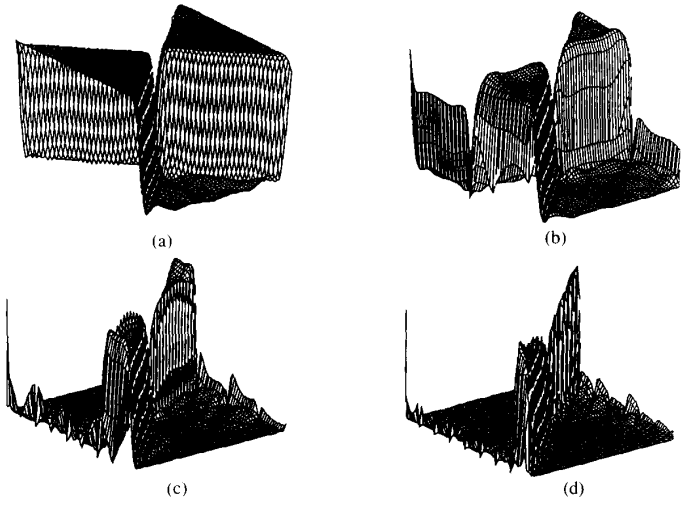

Fig. 14. Frequency responses for 2-band, 4-band, 8-band, and 16-band systems.

sixteen directional subband components of the Cameraman image are shown in Fig. 15. An interpolated version of one of the directional outputs is shown in Fig. 16. The directional information is clearly visible in the interpolated channel and thus provides a more intuitive representation. When all interpolated channels are summed together, the original image is reconstructed. Furthermore, since the directional filter bank is implemented with the all-pass polyphase filters, the reconstructed image is exactly the same as the original, i.e., no distortion is introduced.

In summary, a new filter bank for the directional decomposition of multidimensional signals was introduced. Its full value as an analysis/synthesis tool is not known at this time. Preliminary research in specific applications (linear feature enhancement and detection in particular), indicates that gains in both performance and computational efficiency are possible [49]. Several properties of this filter bank lend support to an optimistic forecast of the benefits of the decomposition. First, there is strong evidence [50]–[53] indicating the presence of wide-band directional sensitivity in the cells of the human visual cortex. Thus in applications where one wishes to exploit ori-

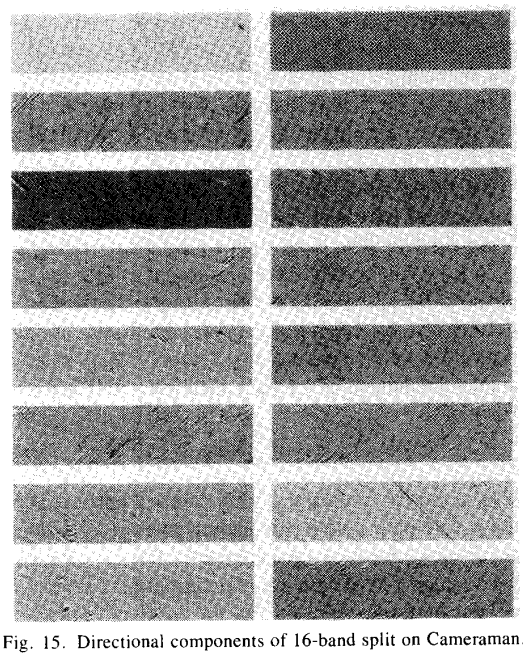

Fig. 15. Directional components of 16-band split on Cameraman.

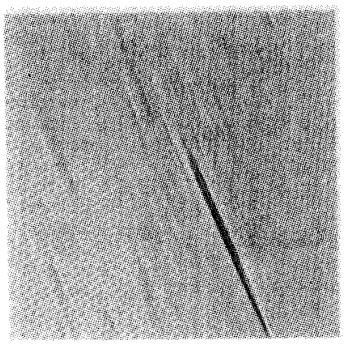

Fig. 16. A single interpolated directional component of the 16-band decomposition of the Cameraman image.

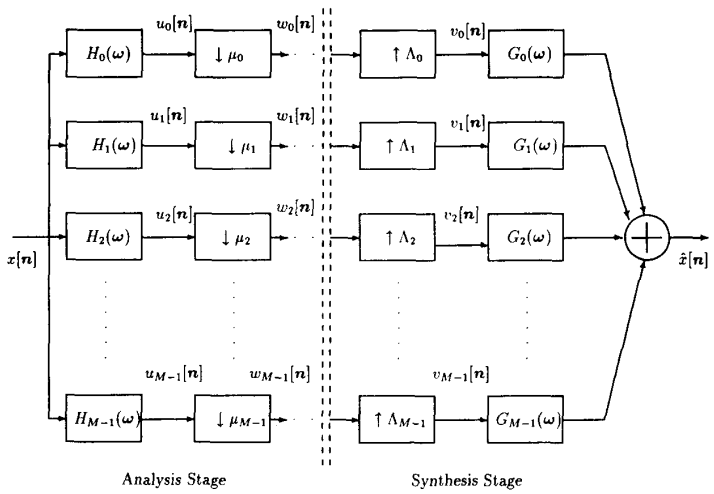

Fig. 17. General filter bank.

entational aspects of visual perception [7], [10], the proposed directional decomposition should be an attractive approach. Second, there are many inherently narrow-band directional decomposition systems which previously have been implemented using transforms such as the Radon [54], Hough [55], [56], Slant-Stack, or Tau-P [26] transforms. These transforms are all related to each other and are based on slices of the two-dimensional Fourier transform of the input image [29]. Most notable is the similarity and relationship between the directional filter bank and the discrete Radon transform or (DRT), details of which can be found in [25]. Thus, the proposed directional filter bank may also be an attractive candidate for applications in which these transforms are employed.

Third, since the directional resolution in the directional filter bank is determined simply by the number of channels, it is a straightforward matter to convert from narrow band to wide band and vice versa. This allows one to easily investigate the range of directional resolutions for traditionally narrow-band and/or wide-band applications. Fourth, the directional analysis/synthesis filter bank can be designed to be both exactly reconstructing and extremely computationally efficient. Thus the filter bank will likely yield analysis/synthesis implementations with higher computational efficiency. Finally, since the proposed filter bank can be maximally decimated, processing can be performed in the decimated signal domain which can significantly improve the computational efficiency with respect to modification of the directional channels. Application of the directional filter bank to specific image processing tasks is presently underway [49].

APPENDIX

The AC matrix theory is a general framework for multirate filter banks. Its two main uses are designing exact and aliasing-free filter banks and analyzing the reconstruction properties of predesigned filter banks. Here the theory is generalized to multidimensional filter banks. In order to extend the AC matrix formulation to a filter bank of the type in Fig. 17, μ_i and Λ_i must be restricted to equal μ for all values of i. (This is the case for the two-band systems used to construct the directional filter bank.) Applying the Fourier properties of the upsamplers and down-

samplers (stated in (4) and (8), respectively) the input/output relationship of the filter bank can be written in a vector/matrix form as

$$\hat{X}(\omega) = \frac{1}{M} G(\omega)^T H_{AC} X(\omega) \tag{41}$$

where

$$\begin{aligned} G(\omega) &= [G_0(\omega) \quad G_1(\omega) \quad \cdots \quad G_i(\omega) \quad \cdots \quad G_{M-1}(\omega)]^T \\ X(\omega) &= [X(\omega) \quad X(\omega - (\mu^T)^{-1} k_1 2\pi) \\ &\quad \cdots \quad X(\omega - (\mu^T)^{-1} k_i 2\pi) \\ &\quad \cdots \quad X(\omega - (\mu^T)^{-1} k_{M-1} 2\pi)]^T \end{aligned} \tag{42}$$

and H_{AC} is the aliasing components matrix whose (i, j) element is $H_i(\omega - (\mu^T)^{-1} k_j 2\pi)$. Therefore, from (41) it follows that the requirement for exact reconstruction is that

$$\frac{1}{M} G(\omega)^T H_{AC} = [D(\omega) \quad 0 \quad \cdots \quad 0]^T \tag{43}$$

where $D(\omega) = z^{-k}$, a spatial shift element. The zeros on the right-hand side of (43) guarantee that all aliasing is canceled. If $D(\omega) \simeq 1$, then near-perfect reconstruction is achieved. (It is also allowable for $D(\omega)$ to approximate a delay.) Given the analysis filters, $H_i(\omega)$, and applying (43), the exact reconstruction synthesis filters are given by

$$\frac{1}{M} G(\omega)^T = [D(\omega), 0 \cdots 0]^T H_{AC}^{-1} \tag{44}$$

where $D(\omega)$ is as previously described.

REFERENCES

[1] D. Petkovic, W. Niblack, and M. Flickner, "Projection based high accuracy measurement of straight line edges," *Machine Vision Appl.*, vol. 1, no. 3, pp. 183-199, 1988.

[2] M. Marra, R. Dunlay, and D. Mathis, "Terrain classification using texture for the ALV," *Proc. SPIE Int. Soc. Opt. Eng.*, pp. 64-70, Nov. 1989.

[3] S. Treitel, J. L. Shanks, and C. W. Frasier, "Some aspects of fan filtering," in *The Robinson Treitel Reader*. 1969, pp. 789-800; paper originally presented at the 36th Annu. Int. Meeting SEG, Houston, TX, Nov. 9, 1966.

[4] P. Embree and J. P. Burg, "Wide-band velocity filtering—the pie slice process," *Geophysics*, vol. 28, pp. 948-974, 1963.

[5] J. P. Fail and G. Gray, "Les filtres en eventail," *Geophys. Prosp.*, vol. 11, pp. 131-163, 1963.

[6] N. M. Mitrou, G. I. Stassinopoulos, E. Protonotarious, M. Singh, A. Allidina, and B. Daniels, "Frequency domain separable decomposition of 2-dimensional systems," in *Parallel Processing Techniques for Simulation, Proc. First Euro. Conf.*, 1986, pp. 95-112.

[7] E. Peli, "Adaptive enhancement based on a visual model," *Opt. Eng.*, vol. 26, pp. 655-660, July 1987.

[8] L. M. Murphy, "Linear feature detection and enhancement in noisy images via the Radon transform," *Patt. Recog. Lett.*, vol. 4, pp. 279-284, Sept. 1986.

[9] G. Hall, T. J. Terrel, J. M. Senior, and L. M. Murphy, "Transputer implementation of the Radon transform for image enhancement," in *Proc. Int. Conf. Acoust., Speech, Signal Processing*, May 1989, pp. 1548-1551.

[10] M. Kunt, "Recent results in high-compression image coding," *IEEE Trans. Circuits Syst.*, vol. CAS-34, pp. 1306-1336, Nov. 1987.

[11] M. Kunt, A. Ikonomopoulos, and M. Kocher, "Second generation image coding techniques," *Proc. IEEE*, vol. 73, pp. 549-574, Apr. 1985.

[12] E. H. Adelson and E. Simoncelli, "Orthogonal pyramid transforms for image coding," *Proc. SPIE Int. Soc. Opt. Eng.*, pp. 50-58, 1987.

[13] E. P. Simoncelli and E. H. Adelson, "Nonseparable extensions of quadrature mirror filters to multiple dimensions," *Proc. IEEE*, pp. 652-664, Apr. 1990.

[14] E. P. Simoncelli and E. H. Adelson, "Nonseparable QMF pyramids," *Proc. SPIE Int. Soc. Opt. Eng.*, pp. 1242-1246, 1989.

[15] B. Mahesh and W. A. Pearlman, "Hexagonal subband coding for images," in *Proc. IEEE Int. Conf. Acoust., Speech, Signal Processing*, pp. 1953-1956, May 1989.

[16] B. Mahesh and W. A. Pearlman, "Image coding on a hexagonal pyramid with noise spectrum shaping," *Proc. SPIE Int. Soc. Opt. Eng.*, pp. 764-774, 1989.

[17] E. Shlomot, Y. Zeevi, and W. A. Pearlman, "The importance of spatial frequency and orientation in image decomposition and coding," in *Visual Communications and Image Processing II*, pp. 152-158, 1987.

[18] J. W. Woods and S. D. O'Neil, "Subband coding of images," *IEEE Trans. Acoust., Speech, Signal Processing*, vol. ASSP-34, pp. 1278-1288, Oct. 1987.

[19] M. J. T. Smith and S. L. Eddins, "Analysis/synthesis techniques for subband image coding," *IEEE Trans. Acoust., Speech, Signal Processing*, vol. 38, pp. 1446-1456, Aug. 1990.

[20] T. Ramstad, "IIR filterbank for subband coding of images," in *Proc. Int. Symp. Circuits Syst.*, 1988, pp. 827-830.

[21] H. Gharavi and A. Tabatabai, "Subband coding of monochrome and color images," *IEEE Trans. Circuits Syst.*, vol. CAS-35, pp. 207-214, Feb. 1988.

[22] P. Westerink, J. Biemond, and D. Boekee, "Subband coding of images using predictive vector quantization," in *Proc. Int. Conf. Acoust., Speech, Signal Processing*, 1987, pp. 1378-1381.

[23] P. Jeanrenaud, "Subband coding of images with recursive allpass filters using vector quantization," master's thesis, Georgia Inst. Technol., Nov. 1988.

[24] D. E. Dudgeon and R. M. Mersereau, *Multidimensional Digital Signal Processing* (Signal Processing Series). Englewood Cliffs, NJ: Prentice-Hall, 1984.

[25] R. H. Bamberger and M. J. T. Smith, "Narrow-band analysis of a filter bank for the directional decomposition of images," in *Proc. IEEE Int. Conf. Acoust., Speech, Signal Processing*, Apr. 1990.

[26] R. H. Tatham, J. Keeney, and I. Nopon, "Application of the Tau-P transform (slant stack) in processing seismic reflection data," preprint of paper presented at 52nd Annu. Meeting SEG, Dallas, TX, 1982.

[27] H. Li and Z. He, "Directional subband coding of images," in *Proc. IEEE Int. Conf. Acoust., Speech, Signal Processing*, May 1989, pp. 1823-1826.

[28] R. Ansari, "Efficient IIR and FIR fan filters," *IEEE Trans. Circuits Syst.*, vol. CAS-34, pp. 941-945, Aug. 1987.

[29] R. M. Mersereau and T. C. Speake, "The processing of periodically sampled multidimensional signals," *IEEE Trans. Acoust., Speech, Signal Processing*, vol. ASSP-31, pp. 188-194, Feb. 1983.

[30] R. Ansari and S. H. Lee, "Two-dimensional multirate processing on nonrectangular grids: Theory and filtering procedures," *IEEE Trans. Circuits Syst.*, submitted for publication.

[31] E. P. Viscito and J. P. Allebach, "The analysis and design of multidimensional FIR perfect reconstruction filter banks for arbitrary sampling lattices," *IEEE Trans. Circuits Syst.*, vol. 38, pp. 29-41, Jan. 1991.

[32] E. Viscito and J. Allebach, "Design of perfect reconstruction multidimensional filter banks using cascaded Smith form matrices," in *Proc. IEEE Int. Symp. Circuits Syst.*, June 1988, pp. 831-834.

[33] G. Karlsson and M. Vetterli, "Theory of two-dimensional multirate filter banks," *IEEE Trans. Acoust., Speech, Signal Processing*, vol. 38, pp. 925-937, June 1990.

[34] M. Vetterli, "A theory of multirate filter banks," *IEEE Trans. Acoust., Speech, Signal Processing*, vol. ASSP-35, pp. 356-372, Mar. 1987.

[35] R. Ansari and C. L. Lau, "Two-dimensional IIR filters for exact reconstruction in tree-structured subband decomposition," *Electron. Lett.*, vol. 23, pp. 633-634, June 1987.

[36] M. J. T. Smith and T. P. Barnwell, "A unifying framework for maximally decimated analysis/synthesis systems," in *Proc. Int. Conf. Acoust., Speech, Signal Processing*, 1985, pp. 521-524.

[37] F. Mintzer, "Filters for distortion free two-band multirate filter banks," *IEEE Trans. Acoust., Speech, Signal Processing*, vol. ASSP-33, pp. 626-630, June 1985.
[38] P. Vaidyanathan, "Quadrature mirror filter banks, *M*-band extensions and perfect reconstruction techniques," *IEEE ASSP Mag.*, vol. 4, pp. 4-20, July 1987.
[39] D. Esteban and C. Galand, "Applications of quadrature mirror filters to band voice coding schemes," in *Proc. Int. Conf. Acoust., Speech, Signal Processing*, 1977, pp. 191-195.
[40] T. Ramstad and O. Foss, "Subband coder design using recursive quadrature mirror filters," in *Proc. EUSIPCO*, 1980.
[41] T. P. Barnwell, "Subband coder design incorporating recursive quadrature filters and optimum adpdm coders," *IEEE Trans. Acoust., Speech, Signal Processing*, vol. ASSP-30, pp. 751-765, Oct. 1982.
[42] M. Vetterli, "Multidimensional subband coding: Some theory and algorithms," *Signal Processing*, vol. 6, pp. 97-112, Apr. 1984.
[43] A. Tabatabai, "Some results on two-dimensional pseudoquadrature mirror filters," *IEEE Trans. Circuits Syst.*, vol. CAS-34, pp. 988-92, Aug. 1987.
[44] G. Wackersreuther, "On two-dimensional polyphase filter banks," *IEEE Trans. Acoust., Speech, Signal Processing*, vol. 34, pp. 192-199, Feb. 1986.
[45] P. P. Vaidyanathan, "Perfect reconstruction QMF banks for two-dimensional applications," *IEEE Trans. Circuits Syst.*, vol. CAS-34, pp. 976-978, Aug. 1987.
[46] R. Ansari and B. Liu, "Efficient sampling rate alteration using recursive (IIR) digital filters," *IEEE Trans. Acoust., Speech, Signal Processing*, pp. 1366-1373, Dec. 1983.
[47] P. Vaidyanathan, P. Regalia, and S. Mitra, "Design of doubly complementary IIR digital filters using a single complex all-pass filter, with multirate applications," *IEEE Trans. Circuits Syst.*, vol. CAS-34, pp. 378-388, Apr. 1987.
[48] G. Karlsson and M. Vetterli, "Extension of finite length signals for subband coding," *Signal Processing*, vol. 17, pp. 161-166, June 1989.
[49] R. H. Bamberger and M. J. T. Smith, "A multirate filter bank approach to the detection and enhancement of linear features in images," in *Proc. 1991 IEEE Int. Conf. Acoust., Speech, Signal Processing*, pp. 2557-2560.
[50] S. Marcelja, "Mathematical description of the response of simple cortical cells," *J. Opt. Soc. Amer.*, vol. 70, pp. 1297-1300, Nov. 1980.
[51] J. G. Daugman, "Uncertainty relation for resolution in space, spatial frequency, and orientation optimized by two-dimensional visual cortical filters," *J. Opt. Soc. Amer. A*, vol. 2, pp. 1160-1169, July 1895.
[52] M. A. Webster and R. L. D. Valois, "Relationship between spatial-frequency and orientation tuning of striate-cortex cells," *J. Opt. Soc. Amer. A*, vol. 2, pp. 1124-1132, July 1985.
[53] D. Regan, "Masking of spatial-frequency discrimination," *J. Opt. Soc. Amer. A*, vol. 2, pp. 1153-1159, July 1895.
[54] J. Radon, "(On the determination of functions from their integrals along certain manifolds)," *Ber. Saechs. Akad. Wiss. Liepzig, Math. Phys.*, vol. 69, pp. 262-277, 1917 (in German).
[55] P. V. C. Hough, "Methods and means for recognizing complex patterns," U.S. Patent 3 069 654, 1962.
[56] R. O. Duda and P. E. Hart, "Use of the Hough transform to detect lines and curves and figures," *Commun. Ass. Comput. Mach.*, vol. 15, no. 1, pp. 11-15, 1972.

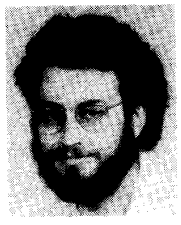

Roberto H. Bamberger (S'87-M'87) was born in Buenos Aires, Argentina, on January 30, 1965. He received the B.E.E. degree in June 1986 and the Ph.D. degree in December 1991, both from the Georgia Institute of Technology.

He is currently an Assistant Professor in the School of Electrical Engineering and Computer Science, Washington State University, Pullman, WA. His research interests include multidimensional signal processing, multirate signal processing, image coding, and image analysis and modeling based on the human visual system.

Dr. Bamberger is a member of Eta Kappa Nu and Tau Beta Pi.

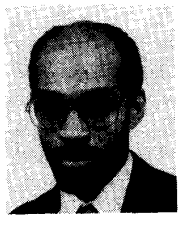

Mark J. T. Smith (S'82-M'82-SM'90) was born in New York, NY, on May 17, 1956. He received the S.B. degree from the Massachusetts Institute of Technology, Cambridge, in 1978 and the M.S. and Ph.D. degrees from the Georgia Institute of Technology, Atlanta, in 1979 and 1984, respectively, all in electrical engineering.

Presently he is an Associate Professor in the School of Electrical Engineering at Georgia Tech. His research interests include speech and image processing, digital filters, filter banks, and time-frequency representations.

Dr. Smith has served as an Associate Editor for the IEEE TRANSACTIONS ON ACOUSTICS, SPEECH, AND SIGNAL PROCESSING, and Coordinator of Local Arrangements for the 1988 Digital Signal Processing Workshop. Presently he is a member of ASSP Digital Signal Processing Technical Committee. He was the recipient of several teaching awards at Georgia Tech and a recent recipient of the 1989 ASSP Paper Award in Speech Processing.